HEAT TRANSFER ANALYSIS
OF A VAPOR-COOLED SHIELD

A Thesis

Presented to

the Faculty of the College of Engineering

The University of Houston

In Partial Fulfillment

of the Requirements For the Degree

Master of Science in Mechanical Engineering

by

Thomas L. Davies

December 1970

ACKNOWLEDGEMENTS

I wish to express my appreciation to the following for their help in preparation of this thesis:

To my employer, The National Aeronautics and Space Administration, for the use of computing facilities and for providing financial support throughout my graduate study.

To my thesis committee for their efforts and in particular to Dr. Richard T. Beaubouef, my advisor, for his guidance and counsel.

To Mr. Harry Cazemier and Mr. Ralph Coldewey for their advice and assistance.

To my wife, Punkie, for her patience and understanding.

HEAT TRANSFER ANALYSIS

OF A VAPOR-COOLED SHIELD

An Abstract of a Thesis

Presented to

the Faculty of the College of Engineering

The University of Houston

In Partial Fulfillment

of the Requirements For the Degree

Master of Science in Mechanical Engineering

---

by

Thomas L. Davies

December 1970

ABSTRACT

A thermal performance analysis of a fin-tube thermal radiation heat shield suspended in the vacuum space between two parallel flat plates is presented. One of the plates is maintained at a constant elevated temperature while the other plate is used as a low temperature sink. This two-dimensional model of a cryogenic Dewar vessel vapor-cooled shield includes consideration of several effects usually neglected in shield analysis. These considerations include local dependence of plate thermal conductivity and emissivity on surface temperature, in addition to the variable fluid properties within the tube. The results of the analysis are used to assess the effectiveness of vapor-cooled shields in reducing the heat transfer from source (Dewar outer shell) to sink (Dewar inner shell).

TABLE OF CONTENTS

LIST OF FIGURES

Figure Page

NOMENCLATURE

a	absorptivity
A	area
C	capacitor
C_p	specific heat
d	differential operator
D	diameter of tube
e	emissivity
F	shape factor; Fahrenheit
G	conductance
h	surface film coefficient
k	thermal conductivity
L	length of fin
$\dot{m}$	mass flowrate
Nu	Nusselt number
P	fluid density
Pr	Prandtl number
Q	energy transfer
Re	Reynolds number
S	Stefan-Boltzmann constant, 0.1712×10^{-8} BTU/HR-FT^2-$^{\circ}$R^4
t	fin thickness
T	temperature
u	dynamic viscosity

V	fluid velocity
W	fin width
x	axis perpendicular to tube in plane of fin
y	axis perpendicular to tube normal to plane of fin
z	axis parallel to tube in plane of fin

Subscripts

f	fluid
F	fin or shield
h	surface film
H	source or Dewar outer shell
l	laminar
L	sink or Dewar inner vessel
t	turbulent
x	x-direction
y	y-direction
z	z-direction

CHAPTER I

INTRODUCTION

According to Barron [1]*, the field of cryogenics involves temperatures below -240° F. This dividing line is based on the fact that the normal boiling points of the so-called permanent gases, such as helium, hydrogen, neon, nitrogen, oxygen and air lie below -240° F, while most common refrigerants boil at temperatures above -240° F.

The age of cryogenics began in 1877 when Caillete in France first produced a fog of liquid-air droplets and Pictet in Geneva succeeded in producing a small jet of liquid oxygen.

Heat transfer from the warm ambient temperature surroundings was one of the most acute problems encountered by early investigators, because the cryogenic fluids could be retained only a day or two before the liquids boiled away. In order to increase the storage lifetime of the cryogenic liquids, the Polish scientists at the Cracow University Laboratory devised an ingenious technique called vapor-shielding in which the boil-off vapors from the primary cryogenic storage container are utilized to intercept a portion of the incoming heat from the ambient temperature environment. A sketch of this concept is shown in Figure 1. The utilization of the vapor-shielding concept in conjunction with the double walled vacuum annulus

---

* Numbers in brackets denote references listed in Bibliography

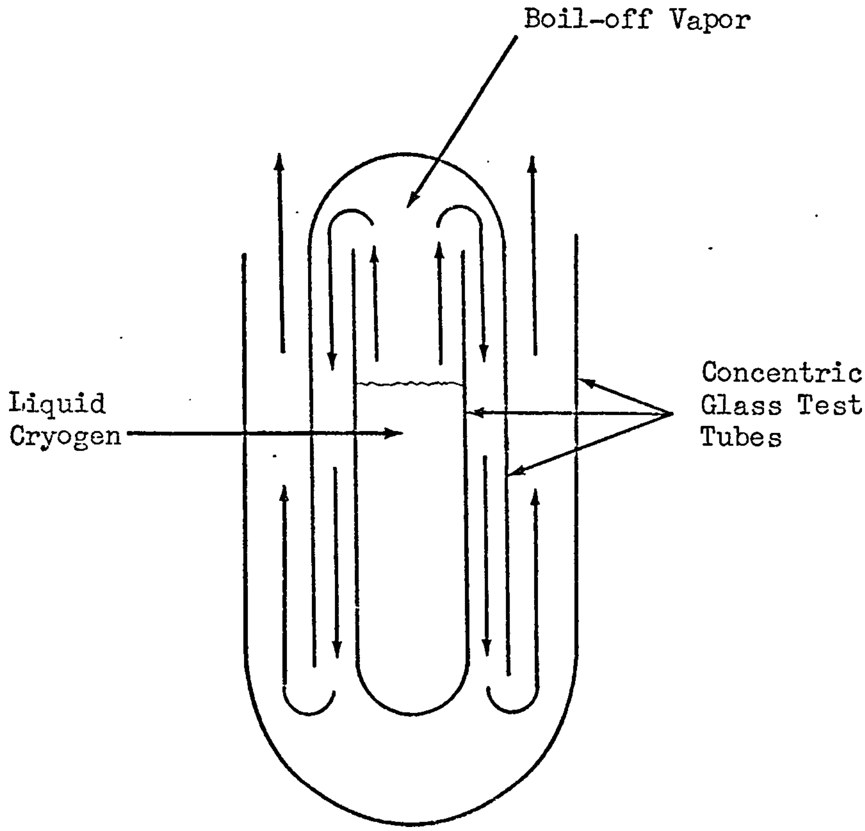

Figure 1. Basic Vapor-Shielding Concept

vessel having silver inner surfaces developed by Sir James Dewar in 1892 is one of the most promising techniques available today for the long term storage of cryogenic liquids. A typical Dewar storage vessel with a vapor-cooled shield is shown schematically in Figure 2.

Although vapor-cooled shields have been used in many existing Dewar cryogenic storage vessels, the shield designs were based on experimental data or simplifying assumptions were made that reduced the scope of analysis to a one-dimensional fin with temperature independent properties.

A review of the literature reveals that significant effort has been directed toward the analysis of thin fin-tube radiators designed to reject heat in a vacuum to a low temperature sink. Lieblien [2] provided one of the early analytical efforts on the temperature distribution and radiant heat transfer for a rectangular fin of constant thickness radiating to deep space. Sparrow, Jonsson, and Minkowycz [3] considered the effects of longitudinal heat conduction in a fin, and the effect of variable thermal properties on one-dimensional heat transfer in radiating fins was investigated by Stockman and Kramer [4].

However, little is known about the heat transfer characteristics of a vapor-cooled shield such as is found in a Dewar vessel. The shield is suspended in the Dewar vacuum annulus, receives heat on one side from the warm outer shell, rejects heat on the other side to the inner pressure vessel which contains the stored cryogenic fluid and is refrigerated by the cold boil-off vapor which is routed to the shield from the pressure vessel vent port. The cold vapor absorbs heat from the shield and is then discharged through an exit

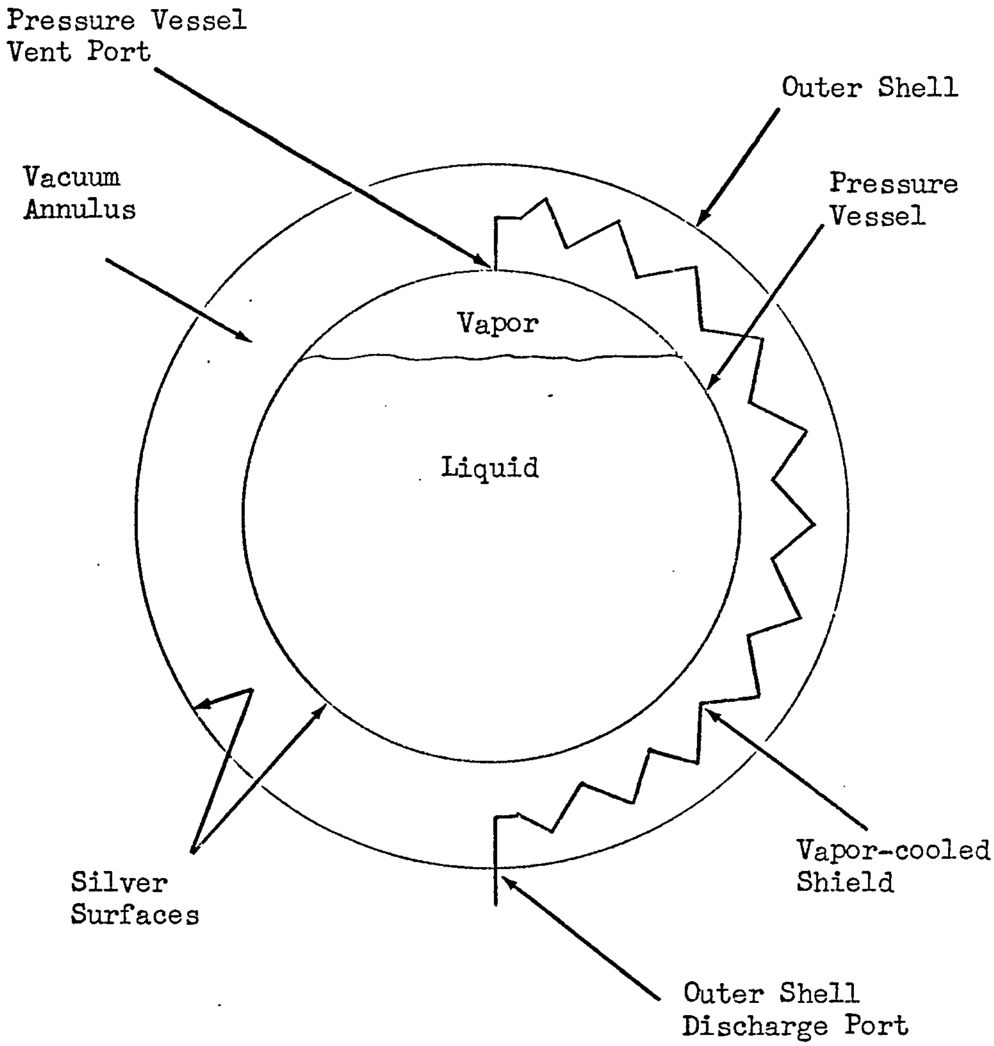

Figure 2. Dewar Vessel with a Vapor-cooled Shield

port in the outer shell. Present analytical techniques do not provide an accurate prediction of the heat transfer from the fin to the fluid in the vapor-cooled shield tube. The routing of the tube on the shield is usually dictated by manufacturing convenience. The effectiveness of the shield in reducing the heat leak into the Dewar vessel is normally lumped into the overall tank thermal performance which is usually measured by the quantity of fluid that boils off per unit time while the tank is in a temperature controlled chamber.

The lack of understanding about the heat transfer characteristics of a vapor-cooled shield is a severe limitation to the designer of high performance (i.e., low fluid loss rate) Dewar cryogenic vessels.

The basic aim of this thesis is to provide a two-dimensional analytical model which can be used to predict the heat transfer characteristics of a Dewar vapor-cooled shield. Of particular interest is the temperature distribution in the fin and the fluid and the rate at which heat is absorbed by the fluid as it progresses through the vapor-cooling tube.

CHAPTER II

FORMULATION OF ANALYTICAL MODEL

This chapter includes the formulation of the two-dimensional flat plate analytical model of a spherical vapor-cooled shield suspended in the vacuum annulus of a Dewar vessel. A qualitative estimate of the degree of conservatism inherent in the model for determining the axial heat absorption profile of the fluid within the vapor-cooling tube is also presented.

The Dewar vapor-cooled shield shown schematically in Figure 2 is depicted pictorially in Figure 3. The fluid enters the vapor-cooling tube at the top of the spherical shield, traverses the shield surface in a helical pattern toward the bottom of the sphere at which point the tube leaves the shield surface and is routed to the outer shell discharge port. The same vapor-cooled tube routing is shown for a flat projection of the spherical shield in Figure 4. This flat projection of the spherical shield may then be approximated with the rectangular flat plate fin-tube shield shown in Figure 5.

In order to accurately describe the flat plate model of the spherical vapor-cooled shield, appropriate reader-perspective must be provided. It is assumed that the rectangular flat plate fin-tube shield is suspended between two parallel flat plates as shown in Figure 6. Heat transfer by conduction from plate to plate and plate to shield is neglected.

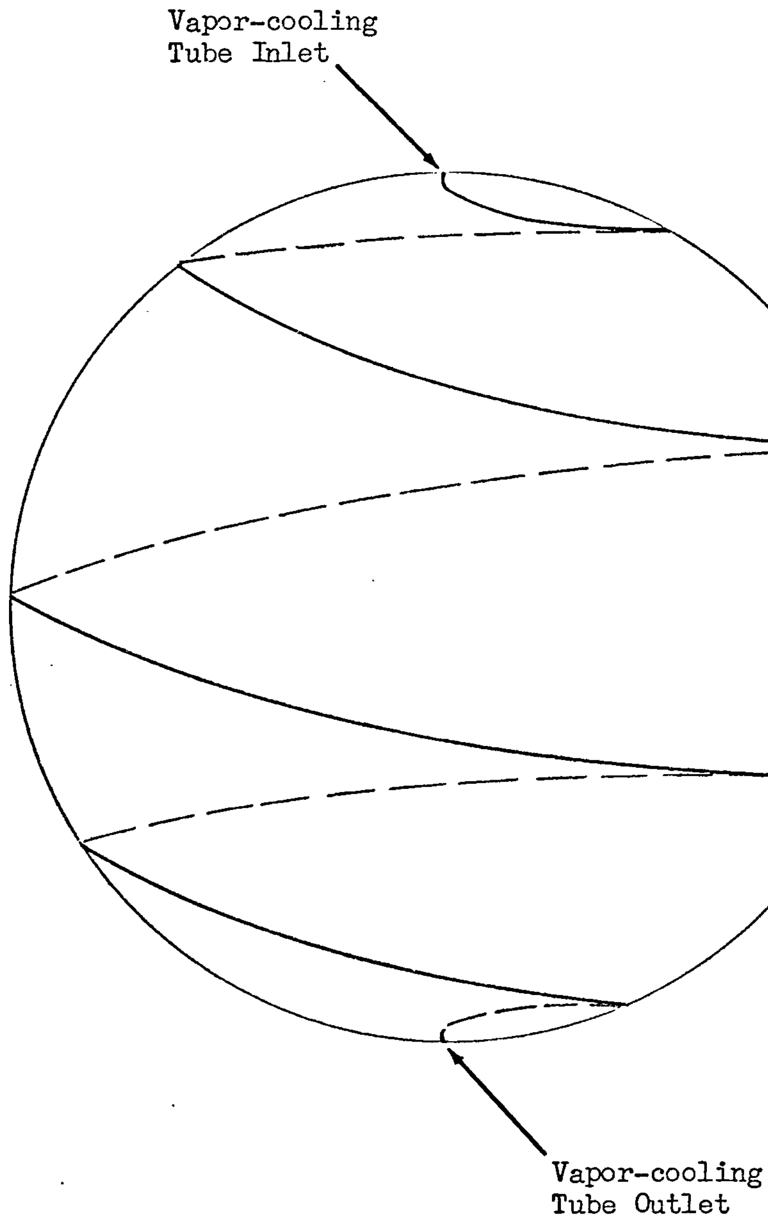

Figure 3. Spherical Vapor-cooled Shield

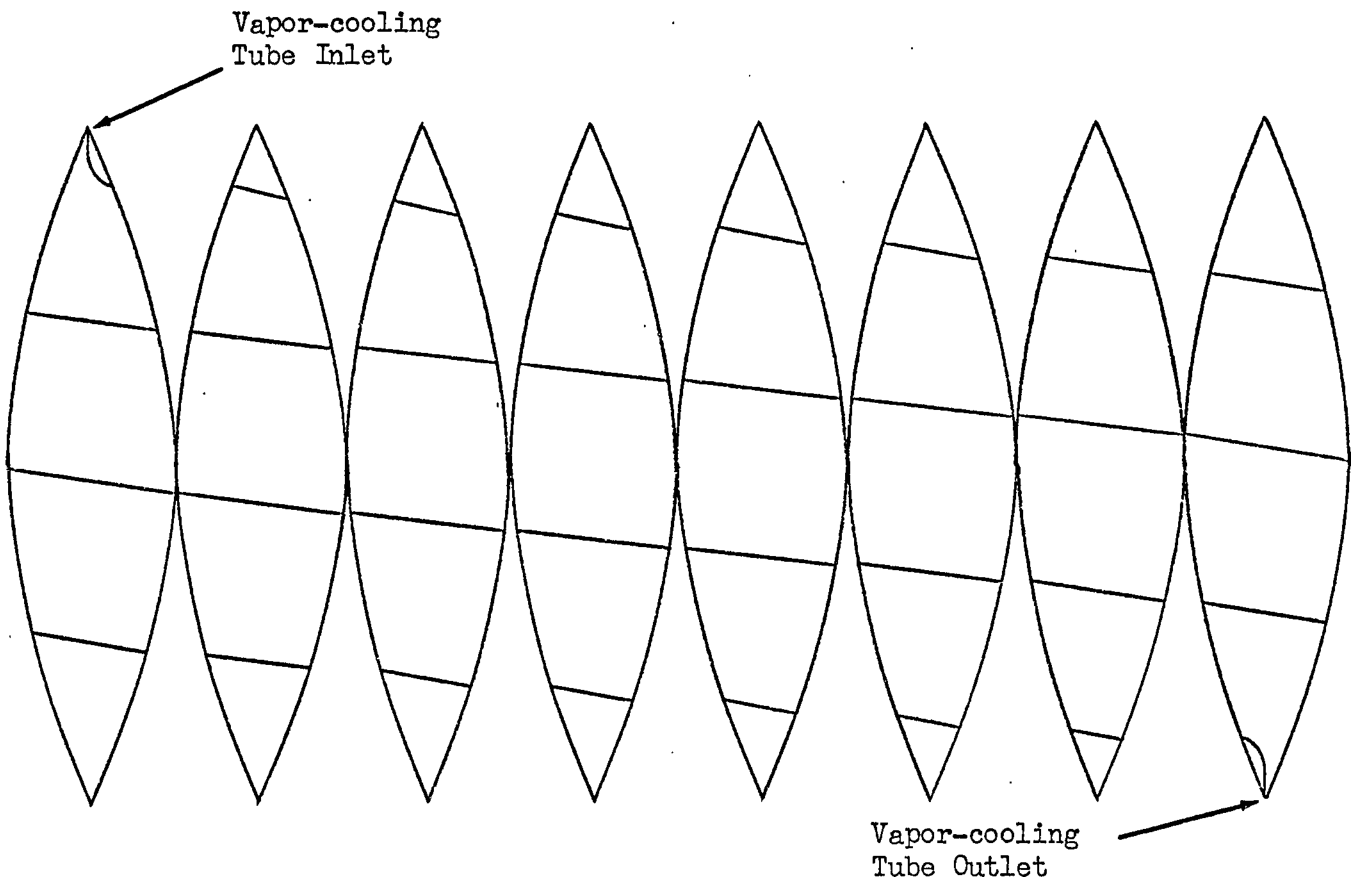

Figure 4. Flat Projection of Spherical Vapor-cooled Shield

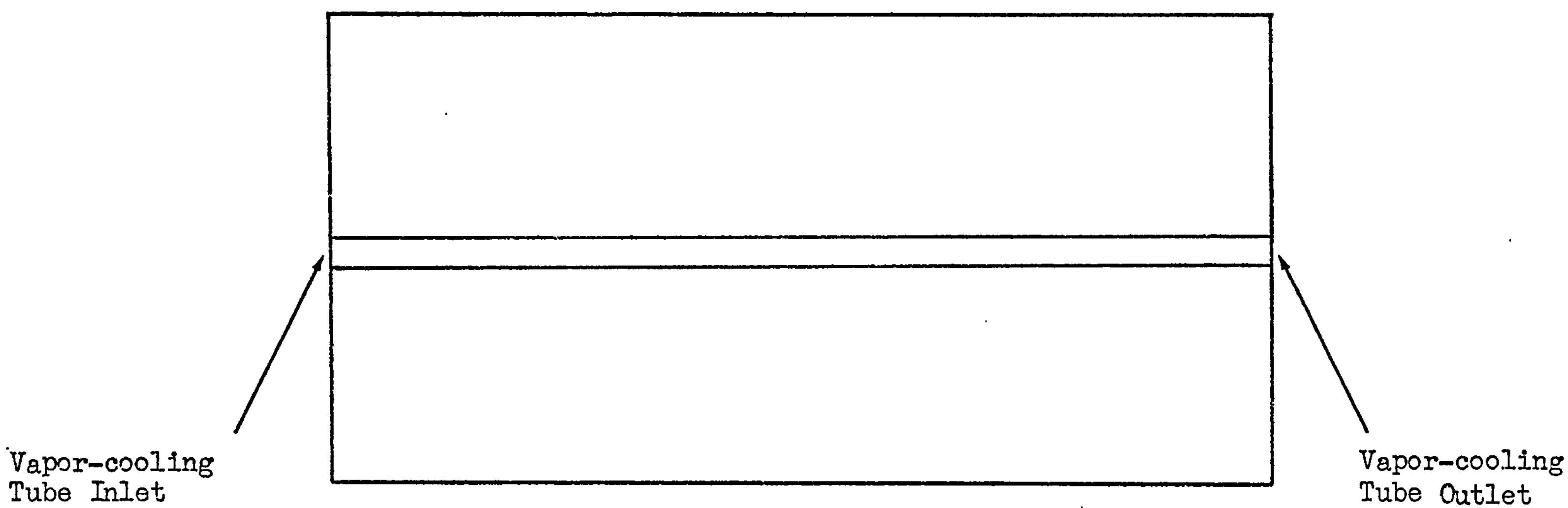

Figure 5. Rectangular Flat Plate Fin-tube Shield Model

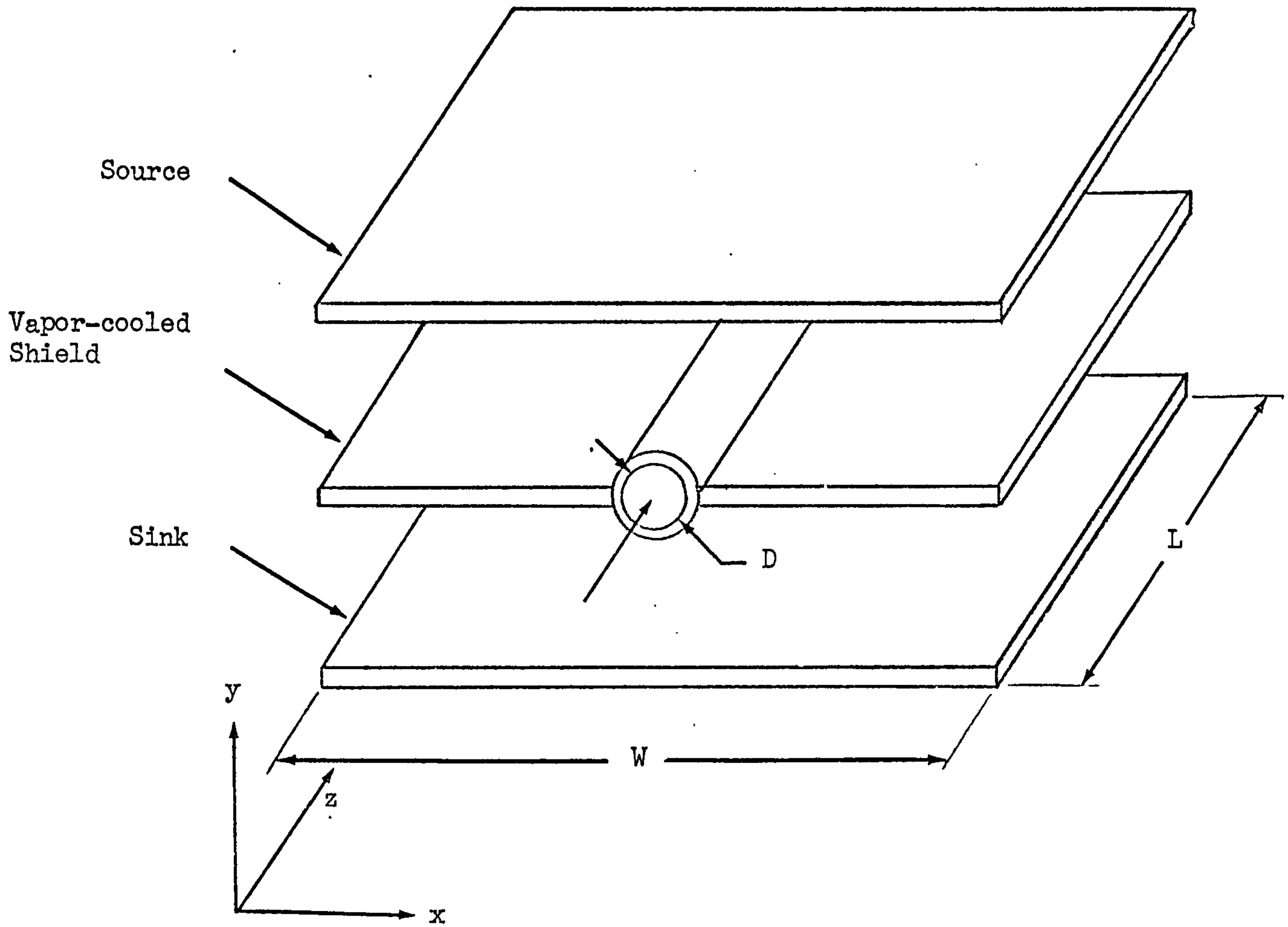

Figure 6. Two-dimensional Model of a Dewar Vessel with a Vapor-cooled Shield

Since the space between the plates is assumed to be an evacuated vacuum annulus, the heat transfer by convection may also be neglected. For clarity, during the remainder of this paper, the outer shell of the Dewar vessel represented in the model by the warm upper plate will be referred to as the source; the vapor-cooled shield will be called the fin-tube shield and the inner pressure vessel represented by the lower plate will be designated as the sink. The source and sink are assumed to be finite parallel opaque and diffusely-radiating surfaces. All surfaces will be taken as both diffuse and gray.
By definition according to Howell and Siegel [5], when a surface is diffuse-gray, the directional spectral emissivity and absorptivity do not depend an either angle or wavelength, but can depend on temperature. As a result of this definition, at any surface temperature T the hemispherical total absorptivity and emissivity are equal and depend only on T; i.e., $a(T) = e(T)$. Even though this behavior is approached by only a limited number of real materials, the diffuse-gray approximation is often made to simplify greatly the radiation analysis. Jakob [6] indicates that if the source, fin-tube shield and sink are very large and closely spaced parallel flat surfaces that the edge effects are negligible when compared to the total exchange of radiation. Thus the shape factor, F, between the surfaces approaches unity. The fin is assumed to be sufficiently thin and well conducting that the temperature is the same on both sides of the fin-tube shield.

The fin-tube shield width is W, the thickness is t and the length is L. These dimensions are measured in the x, y and z directions respectively. The vapor-cooling tube of diameter D is located at the center of the fin at $x = W/2$ and extends axially in the z direction the full fin length L.

The source is maintained at a constant temperature, T_H, which corresponds to the nominal temperature of a Dewar outer shell (70° F). The sink is also maintained at a constant temperature, T_L, which is taken as the boiling point of liquid hydrogen at one atmosphere (-423° F). For cases involving vapor flow through the tube, it is assumed that the vapor inlet temperature to the shield will be held constant at the boiling point of hydrogen (-423° F). The fluid temperature, which will change considerably during the course of its passage through the tube as it absorbs heat from the fin, is designated as $T_f(z)$. The exterior surface area of the vapor cooling tube is not considered in radiant heat exchange calculations because the surface area of the tube is small compared to the overall fin area. Thus any part of the vapor-cooling tube that is not in contact with the fin is considered to be adiabatic.

The source and sink surfaces are silver plated and the emissivity, e, of the surfaces is given as a function of temperature for each as $e_H(T)$ and $e_L(T)$; respectively. The aluminum fin of the fin-tube shield is also silver plated and its locally temperature-dependent emissivity is noted as $e_F(T)$. Similarly, the local fin thermal conductivity as a function of temperature is given as $k_F(T)$.

The hydrogen vapor properties may vary continuously from fluid inlet to exit of the tube. The fluid specific heat, dynamic viscosity and thermal conductivity are designated by $C_{pf}(T)$, $u_f(T)$ and $k_f(T)$, respectively.

Consider the operation of the Dewar vessel two-dimensional model. The specific purpose of the fin-tube shield is to intercept a portion of the radiant energy leaving the warm source (70° F) and travelling toward the cold sink (-423° F). A static fin-tube shield (no fluid flow) will reach steady state thermal equilibrium at a temperature value between the source and sink and should reduce the net heat flux to the sink by approximately fifty per cent. If all surfaces are silver plated, the static fin-tube shield temperature should stabilize at approximately 25° F. This value is calculated using temperature-dependent emissivity values for all surfaces involved.

When the cold cryogenic hydrogen vapor is introduced to the shield at the tube inlet ($z = 0$), a significant reduction in net heat transfer to the sink should result. It should be clearly understood that the transient chill-down of the shield from a prior static thermal equilibrium condition to the final steady state flow condition is not included as a portion of this analysis. A two-dimensional steady-state temperature distribution of the fin surface used with the vapor heat absorption and temperature profiles in the tube is required to assess the true effectiveness of vapor cooling on net source-to-sink heat leak reduction.

A theory popular at present is that the hydrogen vapor may warm up very rapidly (within inches from the tube inlet) and reach thermal equilibrium with the shield almost immediately after entering the tube. This type of behavior would indicate that the vapor-cooling tube may be superfluous beyond perhaps the fluid entrance length. One objective of this analysis is an assessment of the validity of the quick-warmup theory, at reasonable conditions. The two-dimensional model chosen will yield a higher (thus conservative) heating rate to the fluid than the spherical shield in a Dewar vessel due to geometric considerations. This conservatism is based on the fact that the two-dimensional fin provides a greater than actual amount of fin surface area per linear section of tubing near the inlet and exit as shown in the following sketch.

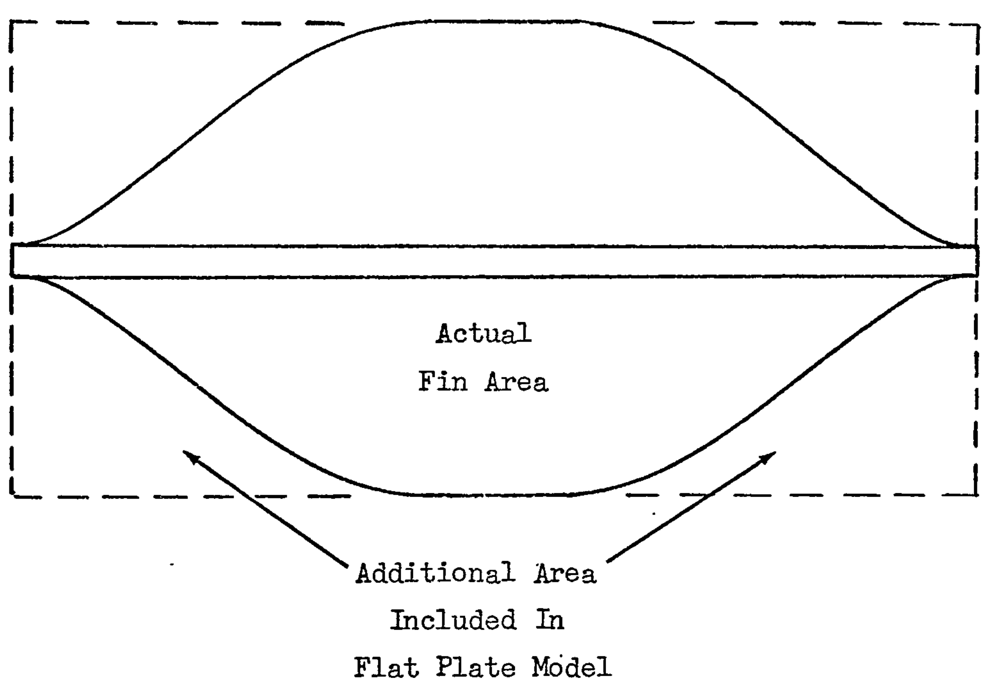

During normal steady state operation, the vapor-cooled shield receives a net quantity of radiant energy from the warm source. A portion of this energy is conducted through the fin to the tube wall and transferred to the cold vapor from the tube wall by forced convection. The fin-tube shield may be considered to be 100 per cent effective if the fluid within the tube can be heated to the temperature of the static shield (i.e., zero flow through the tubing). The length of tubing required for the fluid to achieve thermal equilibrium with the fin is of prime importance to the Dewar vessel design engineer. The net difference between the energy exchange from the source and the fin, and the energy absorbed by the fluid is equal to the net quantity that finally reaches the sink. This may be verified by calculating the net energy exchange between fin and sink during thermal equilibrium and comparing the two values.

The two-dimensional temperature distribution on the fin-tube shield may be determined by applying the energy conservation principle to an elemental cross section of the fin. Under steady-state conditions, the rate of heat flow into the element is equal to the rate of heat flow out of the element; or the sum of the heat conducted into the element in the x and z directions plus the net heat flux from the source to the elemental area is equal to the sum of the heat conducted out of the element at x + dx and z + dz, plus the net heat flux from the elemental area to the sink. In symbolic form, the temperature distribution on the fin surface is given by

$$\frac{d^2T}{dx^2} + \frac{d^2T}{dz^2} = \frac{1}{tk_F(T)}\left\{\frac{T_H{}^4 - T_F{}^4}{\frac{1}{e_H(T)} + \frac{1}{e_F(T)} - 1} - \frac{T_F{}^4 - T_L{}^4}{\frac{1}{e_F(T)} + \frac{1}{e_L(T)} - 1}\right\} S - \frac{1}{k_F(T)}\,\frac{dk_F(T)}{dT}\left[\left(\frac{dT}{dx}\right)^2 + \left(\frac{dT}{dz}\right)^2\right] , \qquad (1)$$

where $T_F = T = T(x, z)$.

An expression for the energy balance on the fluid is also required. For the vapor flowing through the tube, the local value of $T_F(z)$ at the tube wall is related to the local fluid bulk temperature $T_f(z)$ by means of a heat transfer film coefficient h. In turn, the local bulk temperature is determined from an energy balance on the fluid. Thus for a small segment of the tube of length dz, the energy balance may be expressed by the following equation

$$h\,A(T_F(z) - T_f(z)) = \dot{m}C_{pf}(T)dT_f(z) , \qquad (2)$$

where

A = inner surface area of tube segment ;

m = vapor flowrate .

Solutions of the governing equations, (1) and (2), were obtained numerically for several values of the geometrical and flow parameters. The development of a numerical analyzer was not one of the goals of this effort; therefore, an existing numerical analysis computer program was utilized to solve for the temperature distribution and fluid energy balances. The specific details of CINDA (Chrysler Improved Numerical Differencing Analyzer) are provided in [7].

CHAPTER III

METHOD OF SOLUTION

The key to utilizing a network type analysis program such as CINDA lies in the user's ability to develop a lumped parameter representation of the physical problem. Once this has been accomplished, superimposing the network mesh and numbering the network elements is a reasonably straightforward but laborious task. The program allows the user to uniquely identify any element in the network and modify its value or function during the analysis. This feature is extremely useful in changing the value of a local temperature-dependent property during the relaxation of the network. Another feature of the network is that it has a one-to-one correspondence to the mathematical model as well as the physical model.

The following diagram which displays the lumped parameter representation and network superposition of a one dimensional heat transfer problem provides a brief synopsis of the approach used in setting up the two-dimensional model of the vapor-cooled shield problem.

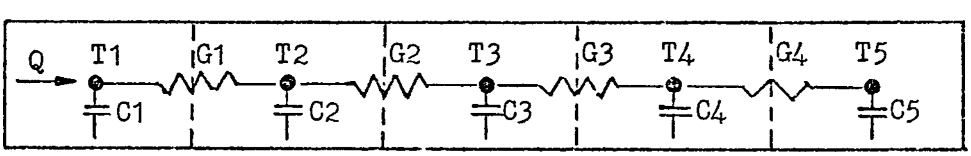

The node points are centered within the lumps and the temperatures are considered uniform throughout each lump. The capacitors shown at the nodes indicate the ability of each lump to store thermal energy. Capacitance values are calculated as the product of lump volume and specific heat. The conductors (electrical symbol G) represent the capability for transmitting thermal energy from one lump to another. Conductor values for energy transmission through solids are calculated as the product of thermal conductivity and heat conduction area divided by the path length (distance between nodes). Conductor values for convective heat transfer are calculated as the film coefficient times the energy cross sectional flow area. Conductors representing energy transfer by radiation are indicated by crossed arrows over the conductor symbols. Radiation heat transfer is non-linear. It is proportional to the difference of the absolute temperatures raised to the fourth power. Utilization of the Fahrenheit system allows automation of this non-linear transfer function by the program and reduces the radiation conductor value to the product of the Stefan-Boltzmann constant times the surface area times the shape factor (taken as unity for this analysis).

There are three types of nodes: diffusion, arithmetic and boundary. Diffusion nodes are those nodes with a positive capacitance and have the ability to store thermal energy. Their future values are calculated by a finite difference representation of the diffusion partial differential equation. Arithmetic nodes are designated by a negative capacitance value. They have no physical capacitance and are unable to store energy. Their future values are calculated by Poisson's partial differential equation. This is a steady state calculation which always utilizes the latest diffusion node values available. Boundary nodes are designated by a minus sign on the node number; they refer to the mathematical boundary, not necessarily the physical boundary. Their values are not changed by the network solution subroutines but may be modified as desired by the user. Boundary nodes are used in this analysis to specify the constant source, sink and fluid inlet temperatures.

The network solution subroutine (known as CINDSS) ignores capacitance values of diffusion nodes to calculate the network steady state solution. The programmer is required to specify the maximum number of iterations to be performed in attempting to reach a steady state solution and the relaxation criteria which determines when it has been reached. For this analysis, the relaxation criteria was that no single node in the entire network could change more than 0.001° F between two successive iterations; a maximum of 100,000 iterations was allowed in search for a steady state solution to the difference equations.

A computer program was used to generate third-order least-squares curve-fit polynomials for all temperature-dependent data used in the analysis. The program included a self-checking subroutine by which the program compares the input data to the value calculated by the polynomial produced; all polynomials are within 5% of the input data. A minimum of 9 and a maximum of 18 data points were used for each of the curve-fit equations; the temperature range for all data was -423° F to $+70^{\circ}$ F.

Thermal conductivity data for the aluminum fin are found in [8]. Emissivity data for the silver surfaces over the temperature range of interest was taken from the unpublished NASA design curve [9] which represents a compilation of over sixty data points from the most current sources available. All of the temperature-dependent property data for gaseous hydrogen at one atmosphere are found in the U. S. Air Force Compendium of Fluid Properties [10].

As indicated previously, there are three basic types of conductors used to join nodes. They correspond to the three modes of heat transfer: conduction, convection and radiation. Conductor values are known as conductances and are calculated using the techniques cited in the one-dimensional fin formulation.

Conduction conductors are used to join all adjacent nodes in the fin. The two-dimensional conduction heat transfer problem is accommodated by using new temperature-dependent conductance values for each relaxation of the fin network. The x-direction (perpendicular to the tube axis) fin conduction conductances are given by

$$G_x = \frac{K(T)\ t\ dz}{dx} \quad ,$$

where

G_x = conductance value for x-direction conductor;

$K(T)$ = temperature dependent fin thermal conductivity curve fit equation;

t = fin thickness;

dz = distance between adjacent nodes in the z-direction;

dx = distance between adjacent nodes in the x-direction;

The z-direction (parallel to the tube axis) fin conductances are similarly given by

$$G_z = \frac{K(T)\ t\ dx}{dz} \quad ,$$

where

G_z = conductance value for z-direction conductor.

The fluid nodes receive heat from each other and from the warm tube wall. The axial fluid nodes are joined by $\dot{m}\ C_p$ conductors. The general form is given by

$$G_f = \dot{m}\ C_{pf}(T) \quad ,$$

where

G_f = conductance value for fluid node-to-fluid node conductor;

$\dot{m}$ = flowrate of hydrogen vapor through tube;

$C_{pf}(T)$ = temperature dependent hydrogen vapor specific heat curve fit equation.

Each fluid node also communicates with a tube wall node on each side of the tube centerline.

The quantity of energy absorbed by the hydrogen gas flowing through the tube of the fin-tube heat shield is approximated by using a local temperature dependent fluid-to-wall conductance value based on the fluid film coefficient.

For the symmetrical geometric model, the general fluid to tube wall convection conductance is

$$G_h = \frac{h(T)\ A}{2} \quad ,$$

where

G_h = conductance value for fluid node to tube wall conductor;

$h(T)$ = temperature and flowrate dependent film coefficient curve fit equation;

$\frac{A}{2}$ = one half of tube inside area per node.

Only half of the tube inside area is used to calculate the heat added to the fluid by convection from each half of the fin.

Care must be taken to use the correct value for the film coefficient since it is possible to have laminar or turbulent flow in the vapor cooling tube.

According to Hendricks, Graham, Hsu and Medieros [11], whenever the fluid follows the perfect gas law and the C_{pf} and transport properties are well behaved, perhaps the best recommendation for correlating local heat transfer in the <u>turbulent</u> flow regime is given by

$$Nu = .023\ Re^{.8}\ Pr^{.4} \quad ,$$

where

Nu = Nusselt Number;

Re = Reynolds Number;

Pr = Prandtl Number.

Recalling that the Nusselt Number, Nu, of the fluid may also be expressed as

$$Nu = \frac{h\ D}{K} \quad ,$$

where

h = fluid film coefficient;

D = tube diameter;

K = temperature dependent fluid thermal conductivity,

it is possible to combine the two expressions for the Nusselt number to yield the following equation for the turbulent flow film coefficient:

$$h_t = .023\ \frac{K(T)}{D} \left(\frac{VDP}{u(T)}\right)^{.8} \left(\frac{u(T)\ C_{pf}(T)}{K(T)}\right)^{.4} \quad ,$$

where

h_t = turbulent flow film coefficient;

$K(T)$ = temperature dependent fluid thermal conductivity curve fit equation;

$u(T)$ = temperature dependent fluid dynamic viscosity curve fit equation;

$C_{pf}(T)$ = temperature dependent fluid specific heat curve fit equation;

D = tube diameter;

V = fluid velocity;

P = fluid density.

A similar expression may be derived for the laminar flow regime and is given by

$$h_l = 1.86\ \frac{K(T)}{D}\left(\frac{VDP}{u(T)}\right)^{.33}\left(\frac{u(T)\ C_{pf}(T)}{K(T)}\right)^{.33}\left(\frac{D}{L}\right)^{.33}$$

where new symbols are

h_l = laminar flow film coefficient;

L = length of vapor cooling tube.

It should be noted that the primary differences between the turbulent and laminar film coefficients are the exponents for the Reynolds and Prandtl numbers, the multiplier (1.86 vs .023) and the tube diameter-to-length ratio.

Transition from laminar to turbulent flow or vice versa was not encountered in any of the cases chosen for analysis. This was checked by calculating the Reynolds number at every fluid node within the tube. The study of transition flow is beyond the scope of this analysis.

Radiation conductance values are calculated using temperature dependent emissivity data. The source-to-fin radiation conductances are given by

$$G_{HF} = \left\{\frac{1}{\frac{1}{e_{H(T)}} + \frac{1}{e_{F(T)}} - 1}\right\} S\ dx\ dz \quad ,$$

where

G_{HF} = source-to-fin radiation conductance;

$e_{H(T)}$ = temperature dependent source emissivity curve fit equation;

$e_{F(T)}$ = temperature dependent fin emissivity curve fit equation;

S = Stefan Boltzmann Constant;

dx = distance between adjacent nodes in x-direction;

dz = distance between adjacent nodes in z-direction;

Similarly we can write

$$G_{FL} = \left\{ \frac{1}{\frac{1}{e_{F(T)}} + \frac{1}{e_{L(T)}} - 1} \right\} S\ dx\ dz$$

where

G_{FL} = fin-to-sink radiation conductance;

$e_{F(T)}$ = temperature dependent fin emissivity curve fit equation;

$e_{L(T)}$ = temperature dependent sink emissivity curve fit equation;

S = Stefan Boltzmann Constant;

dx = distance between adjacent nodes in x-direction;

dz = distance tetween adjacent nodes in z-direction.

The development of the model is directed toward a general solution of a flat plate fin-tube shield. The network is set up to accommodate a broad range of fin sizes and materials. The only limitations are that the fin be sufficiently thin and of high conductivity that ($dT/dy \rightarrow 0$) and that the overall fin size be restricted to allow each node temperature to be representative of the lump. The range of the fin and fluid thermophysical property data that may be used is limited only by the user's imagination. Any combination of sink, source, and fluid inlet temperatures may be used as boundary conditions. As indicated previously, the property data for this analysis is provided as polynomial curve-fit equations to the computer program. A set of test cases was run using the tabular data (used to generate the curve-fit polynomials) and a table look-up interpolation subroutine to obtain the property values as a function of temperature. The results were the same as the curve-fit approach but the amount of computer time doubled. The data interpolation method is simpler to input to the program, since the data curve-fitting step is deleted. However, for a lengthy parametric study involving several shield configurations of the same shield material, the net savings of computer time may justify the extra initial effort. The application requirements of the user should justify the data input approach to be used.

CHAPTER IV

RESULTS AND CONCLUSIONS

Calculations for a representative group of fin configurations were performed on the Univac 1108 computer. The fluid flow rate was varied from 0.00625 to 0.050 lbm/hr. A special case was run for the turbulent flow regime, at 0.20 lbm/hr for L/W = 12.5; see Figure 6 for definitions of L and W. The fin L/W ratio was varied from 0.5 to 50. A total of 17 combinations of mass flow rate and L/W ratio were investigated.

A primary goal of this study was to examine the axial temperature distribution in the vapor. The effect on axial temperature distribution of varying the mass flow rate for 3 fin configurations (holding area constant) is shown in Figures 7, 8, and 9. Similar curves in Figures 10, 11, 12, and 13 show the effect of varying the fin configuration for specific flow rates. The axial fluid temperature distribution is non-linear for relatively low flow rates. As anticipated, the fluid temperature approaches the static shield temperature asymptotically. The curves of Figures 7 through 13 demonstrate the manner in which the vapor approaches thermal equilibrium with the fin, with increasing distance along the tube.

Another effect investigated in this analysis was the local rate of energy absorption by the fluid as a function of distance from the tube inlet. Typical examples of energy-absorption rate are shown

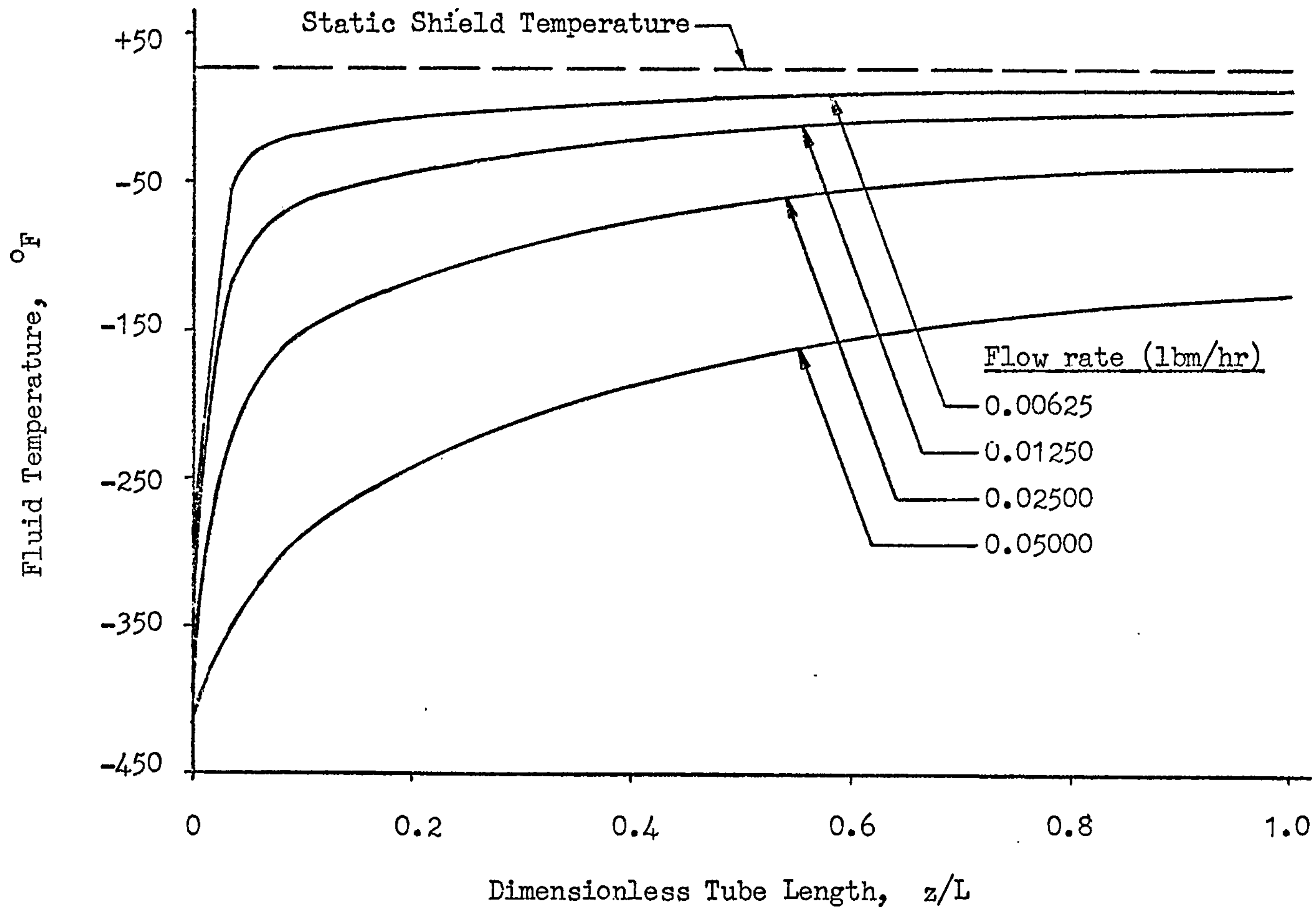

Figure 7. Axial Fluid Temperature Distribution for L/W = 0.5

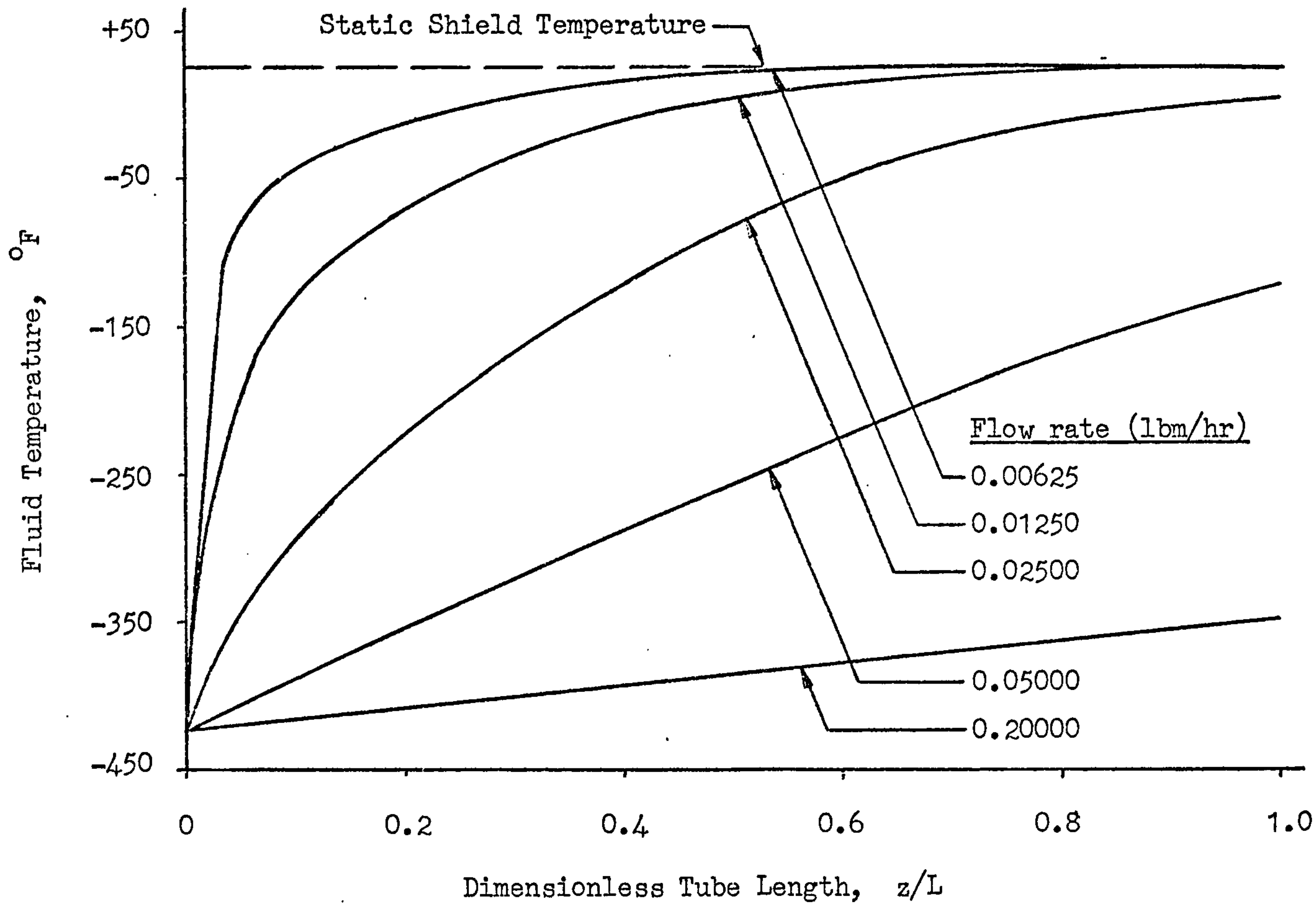

Figure 8. Axial Fluid Temperature Distribution for L/W = 12.5

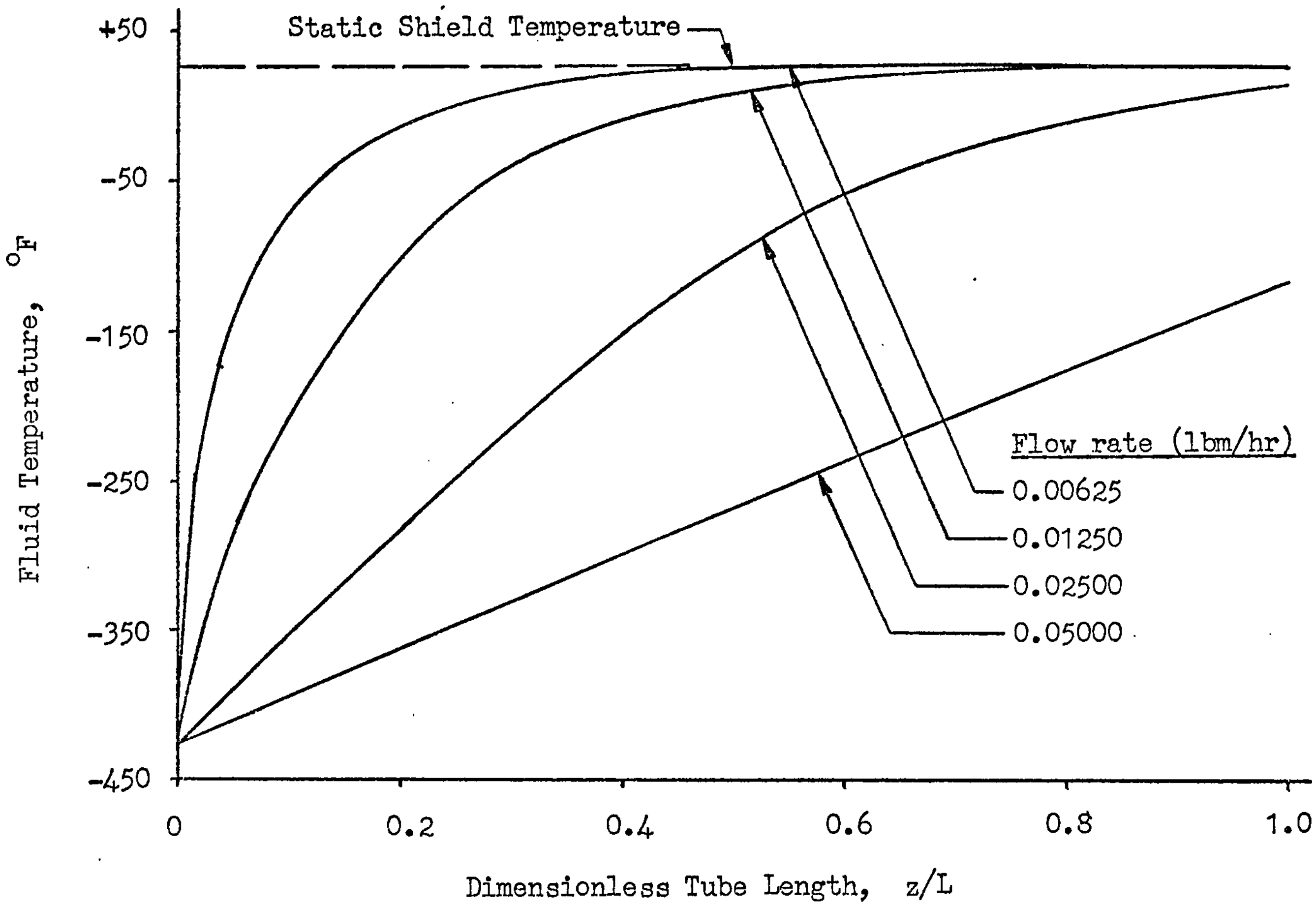

Figure 9. Axial Fluid Temperature Distribution for L/W = 50

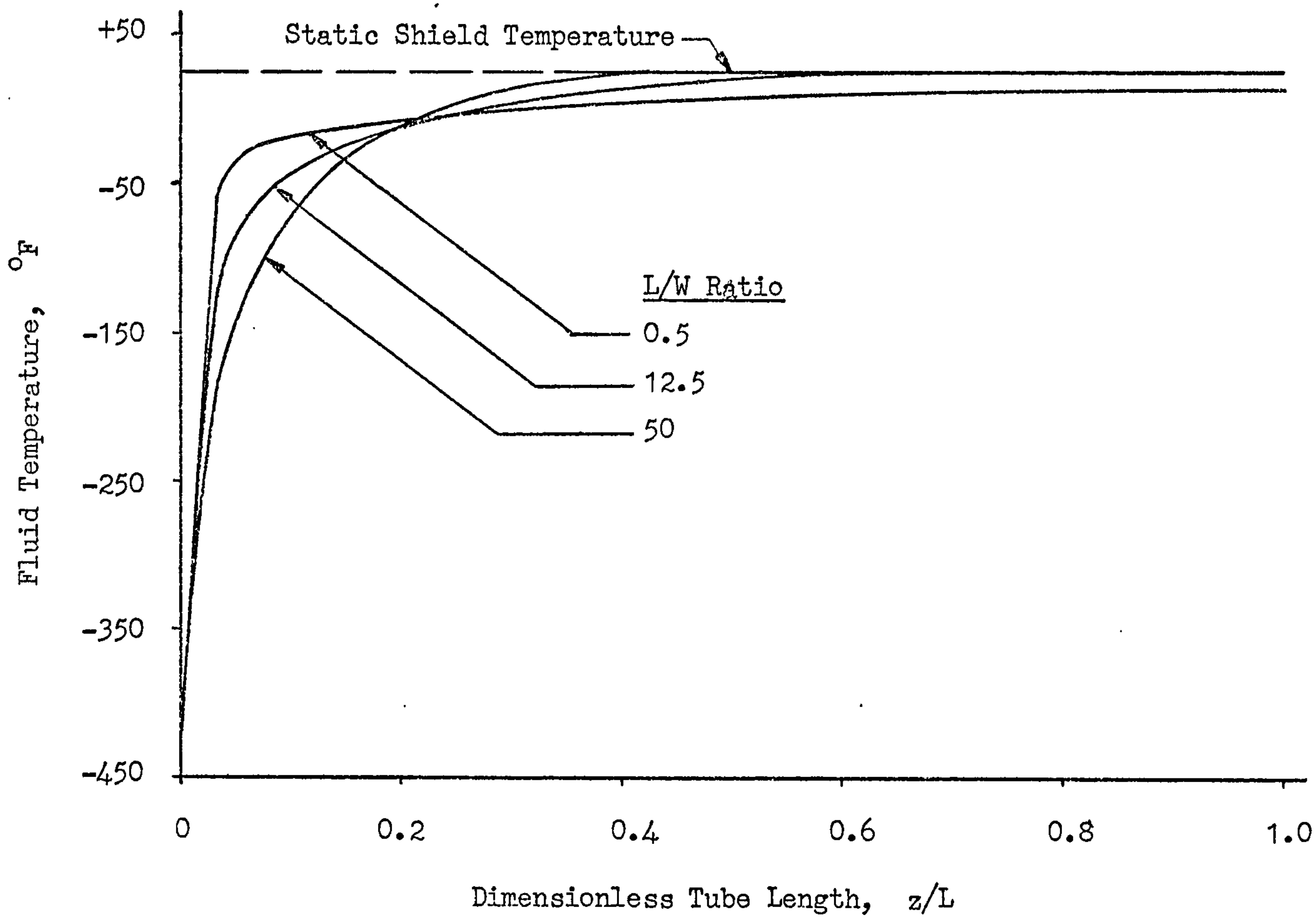

Figure 10. Axial Fluid Temperature Distribution for $\dot{m}$ = 0.00625 lbm/hr

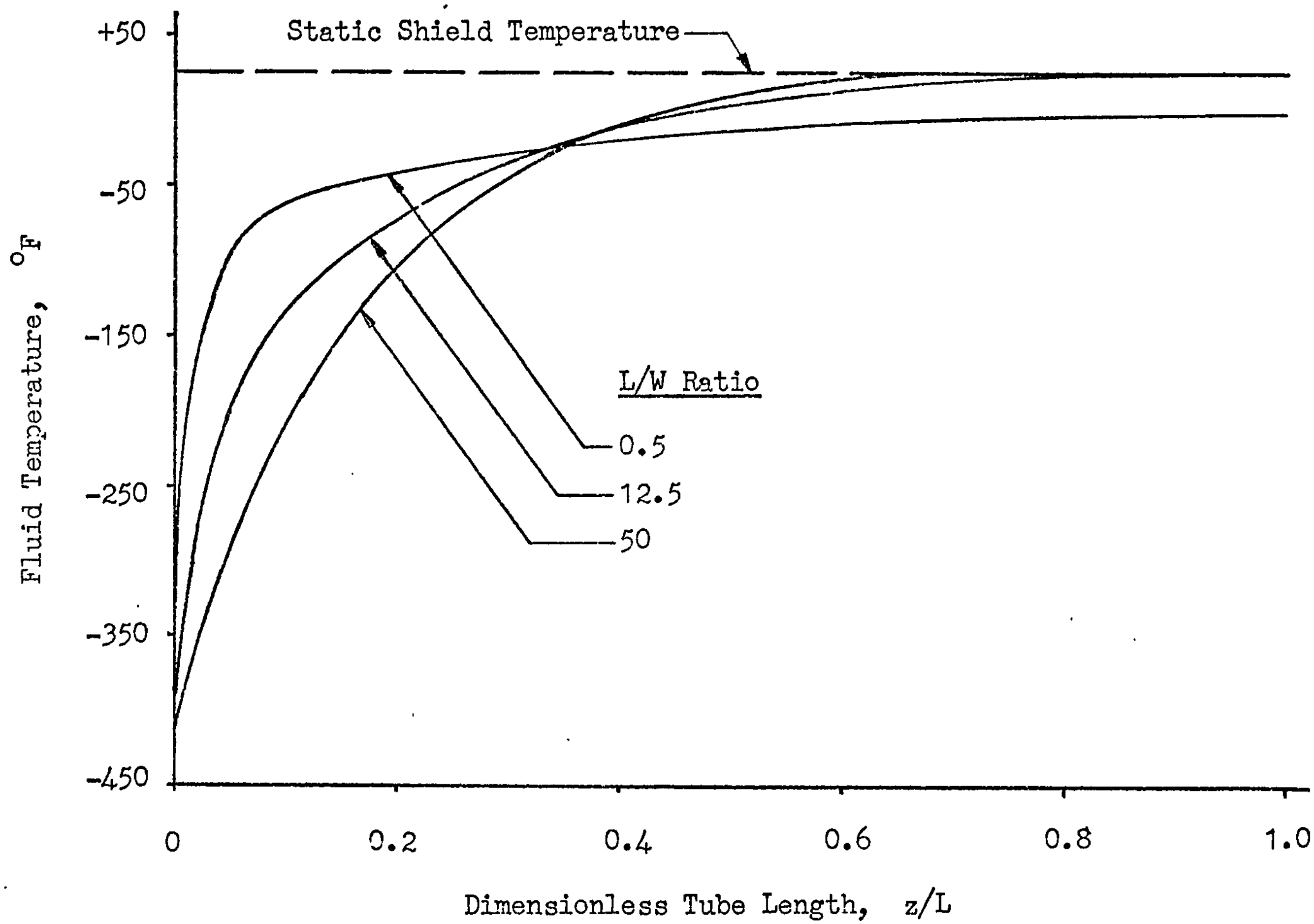

Figure 11. Axial Fluid Temperature Distribution for $\dot{m}$ = 0.01250 lbm/hr

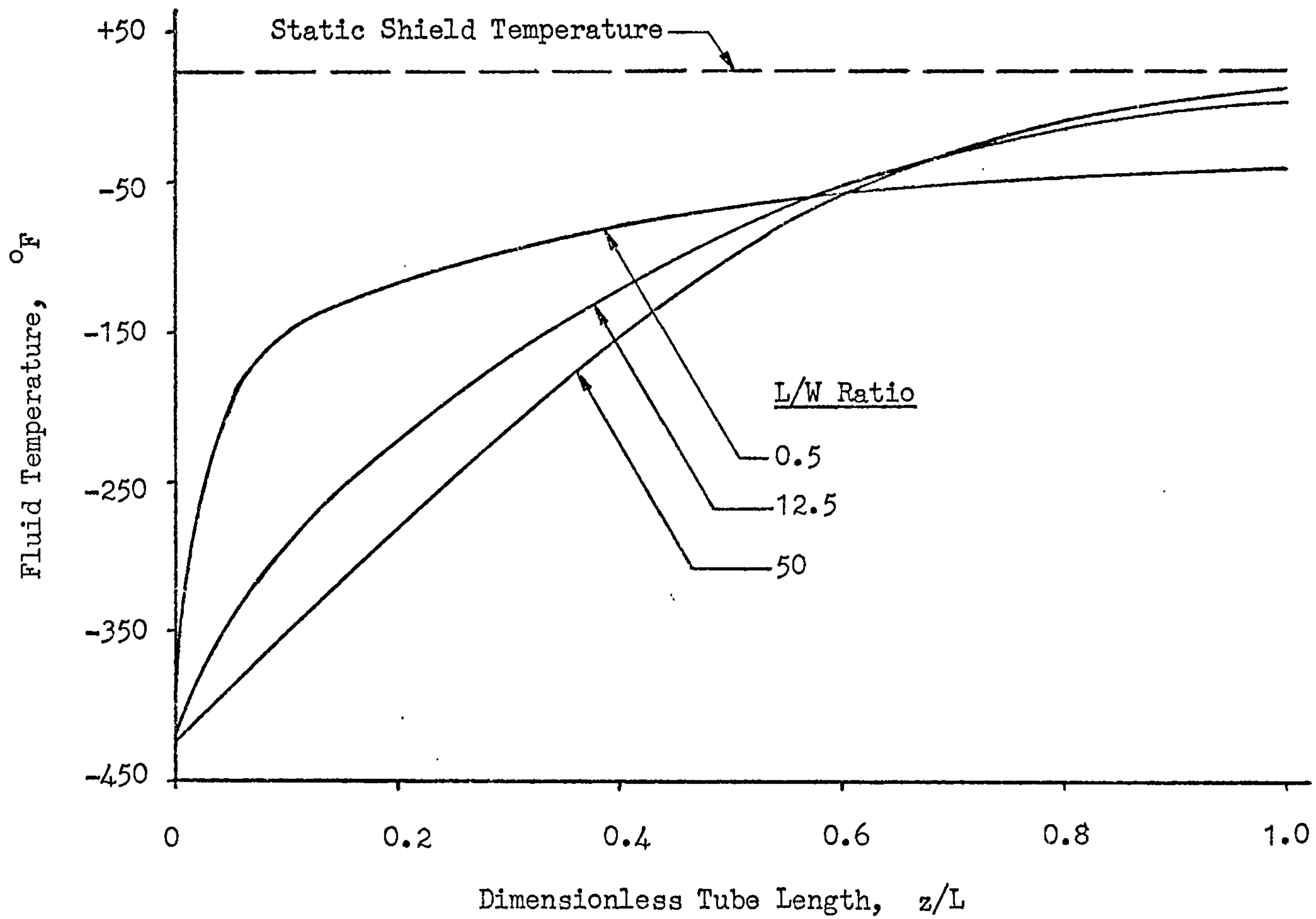

Figure 12. Axial Fluid Temperature Distribution for $\dot{m}$ = 0.0250 lbm/hr

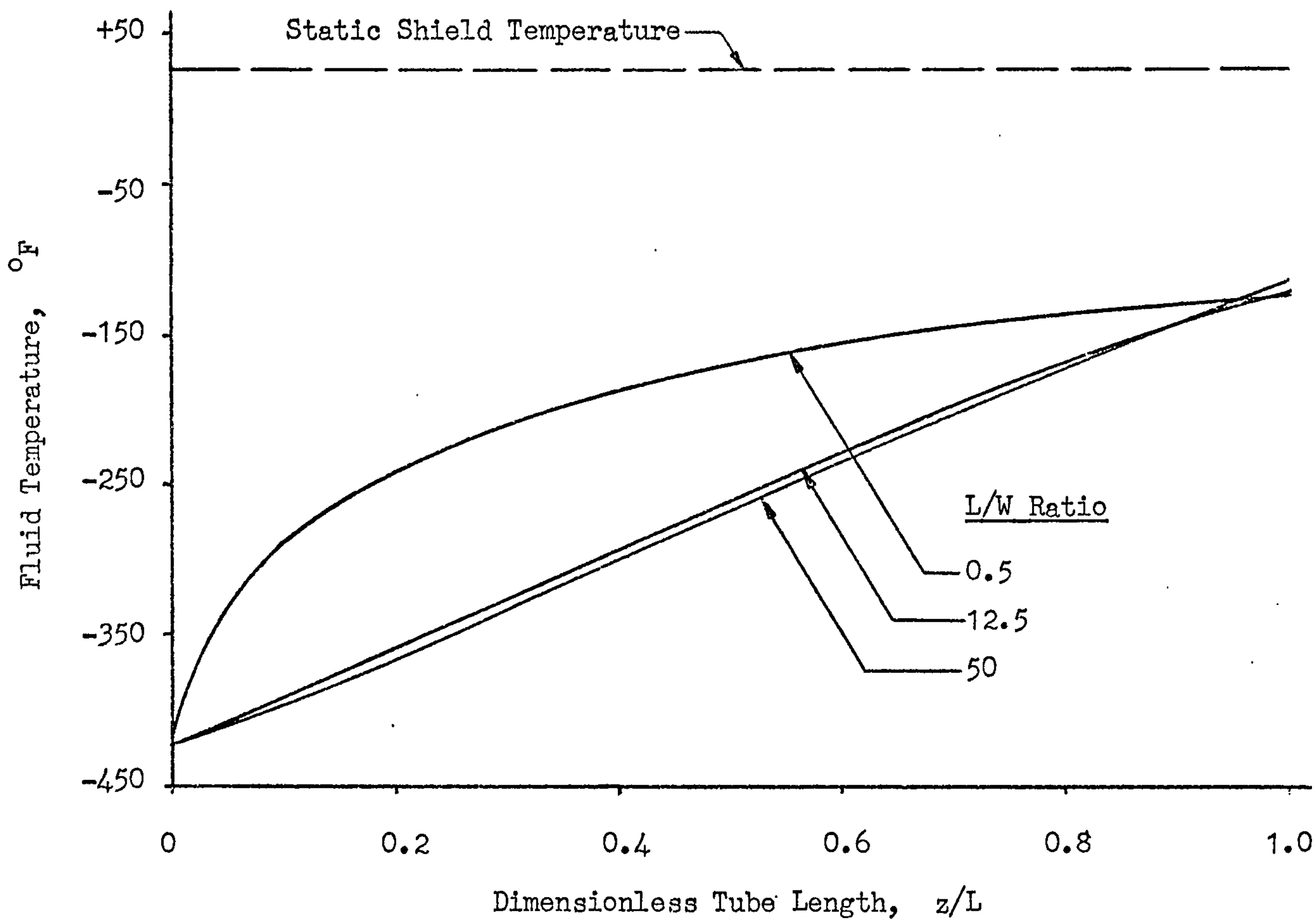

Figure 13. Axial Fluid Temperature Distribution for $\dot{m}$ = 0.0500 lbm/hr

in Figures 14, 15, and 16. The best graphic illustrations of thermal equilibrium between the fluid and the fin are given in Figures 17, 18, and 19. In these three figures the cumulative heat absorbed by the fluid is given as a function of dimensionless length for various flow rates and fin configurations.

The final assessment of shield effectiveness may be made by comparing different values of net heat transfer from fin to sink. In Table 1, values of net heat transfer from fin to sink are shown for the full range of fin configurations and fluid flow rates.

As initially stated, the objective of this thesis was an analytical model capable of predicting the thermal-performance characteristics of a vapor-cooled shield. This objective has been accomplished, within the limitations of the model employed as discussed. The method of analysis utilized will allow the user to approach a vapor-cooled shield analysis effort with confidence.

The quick-warmup theory has some merit for very low flow rates. However, in the nominal range of flow rates (0.025 to 0.05 lbm/hr) for high performance cryogenic fluid-storage vessels, the heat absorption rate of the fluid is reasonably linear as a function of length.

As noted in Table 1, the lowest net heat transfer to sink will result from the highest flow rate and L/W-ratio fin. A minimum heat transfer configuration may or may not be desirable from a design standpoint. The choice of fin configuration and fluid flow rate will be governed by the storage-duration requirement in conjunction with the energy requirement for cryogen vaporization to provide the fluid flow.

Further investigations should be considered for the transition region from laminar to turbulent flow.

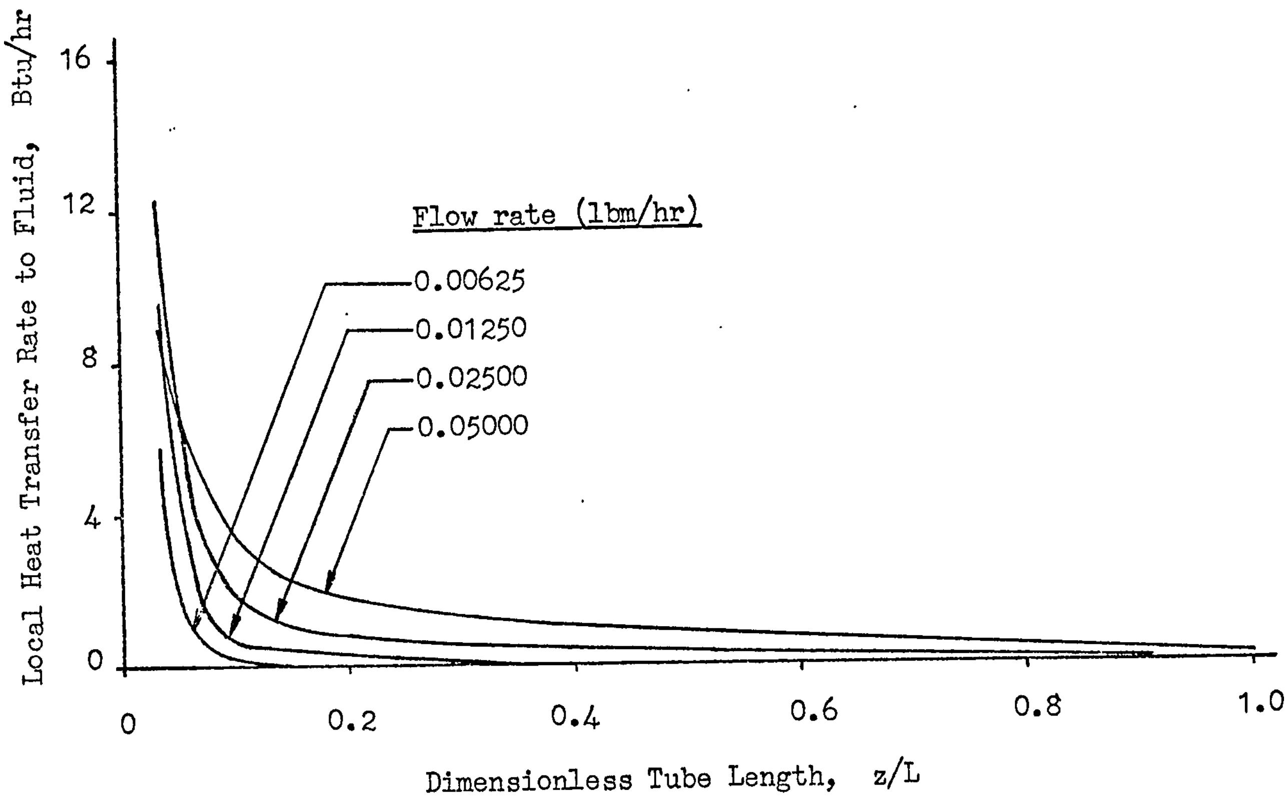

Figure 14. Local Fluid Energy Absorption Profile for L/W = 0.5

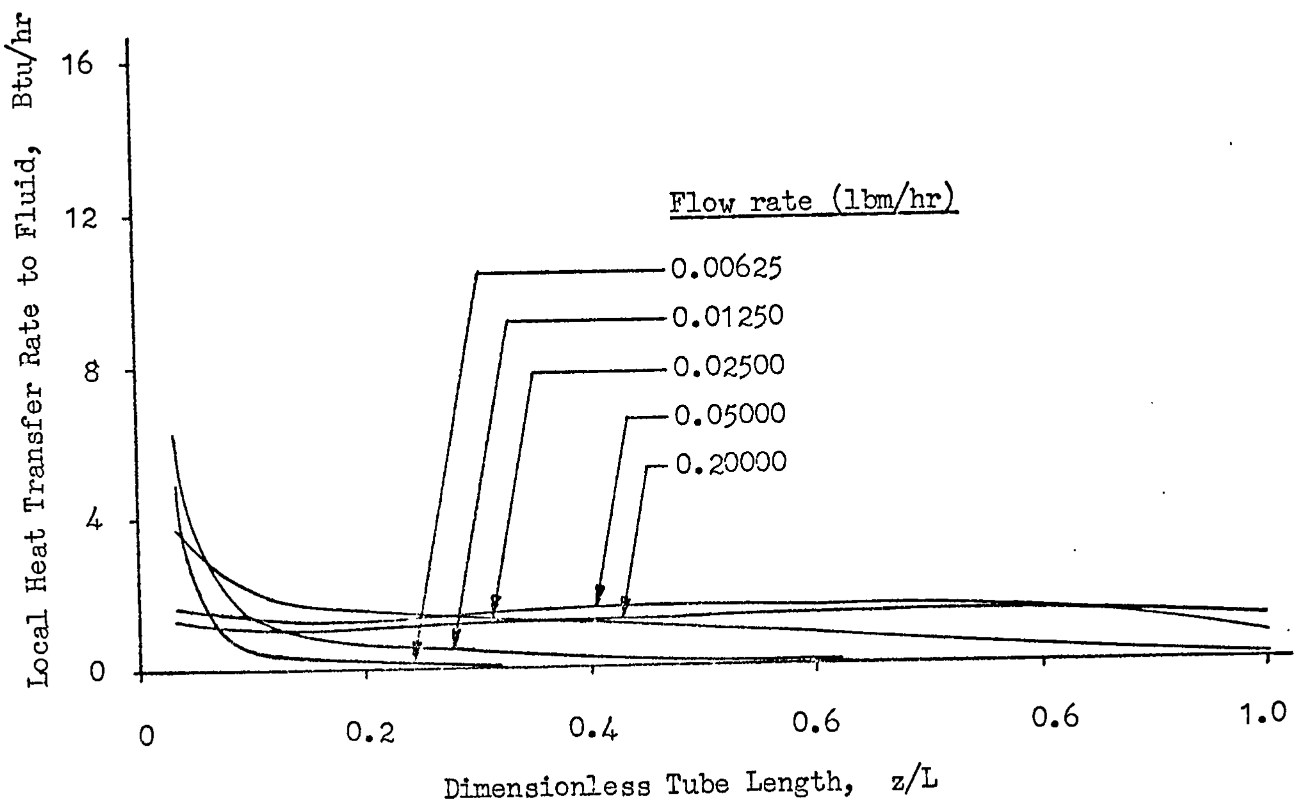

Figure 15. Local Fluid Energy Absorption Profile for L/W = 12.5

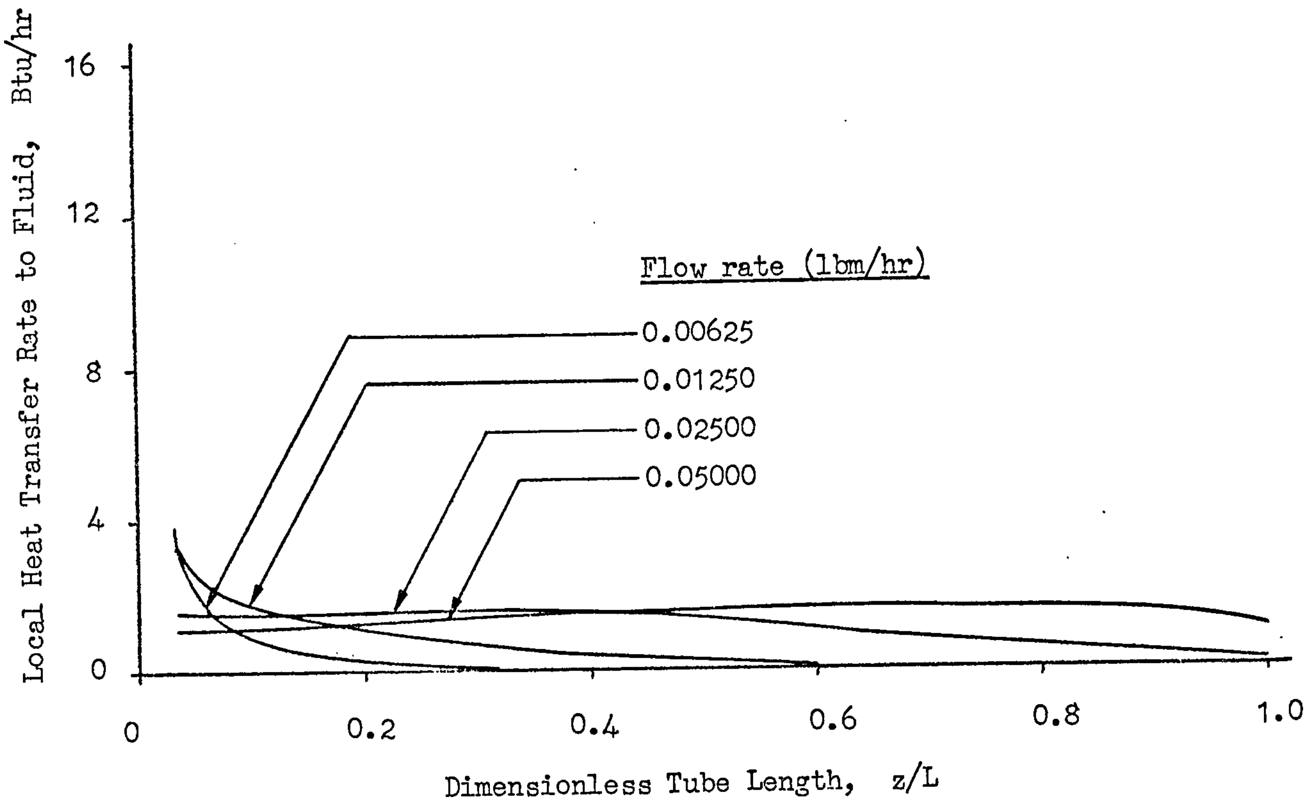

Figure 16. Local Fluid Energy Absorption Profile for L/W = 50

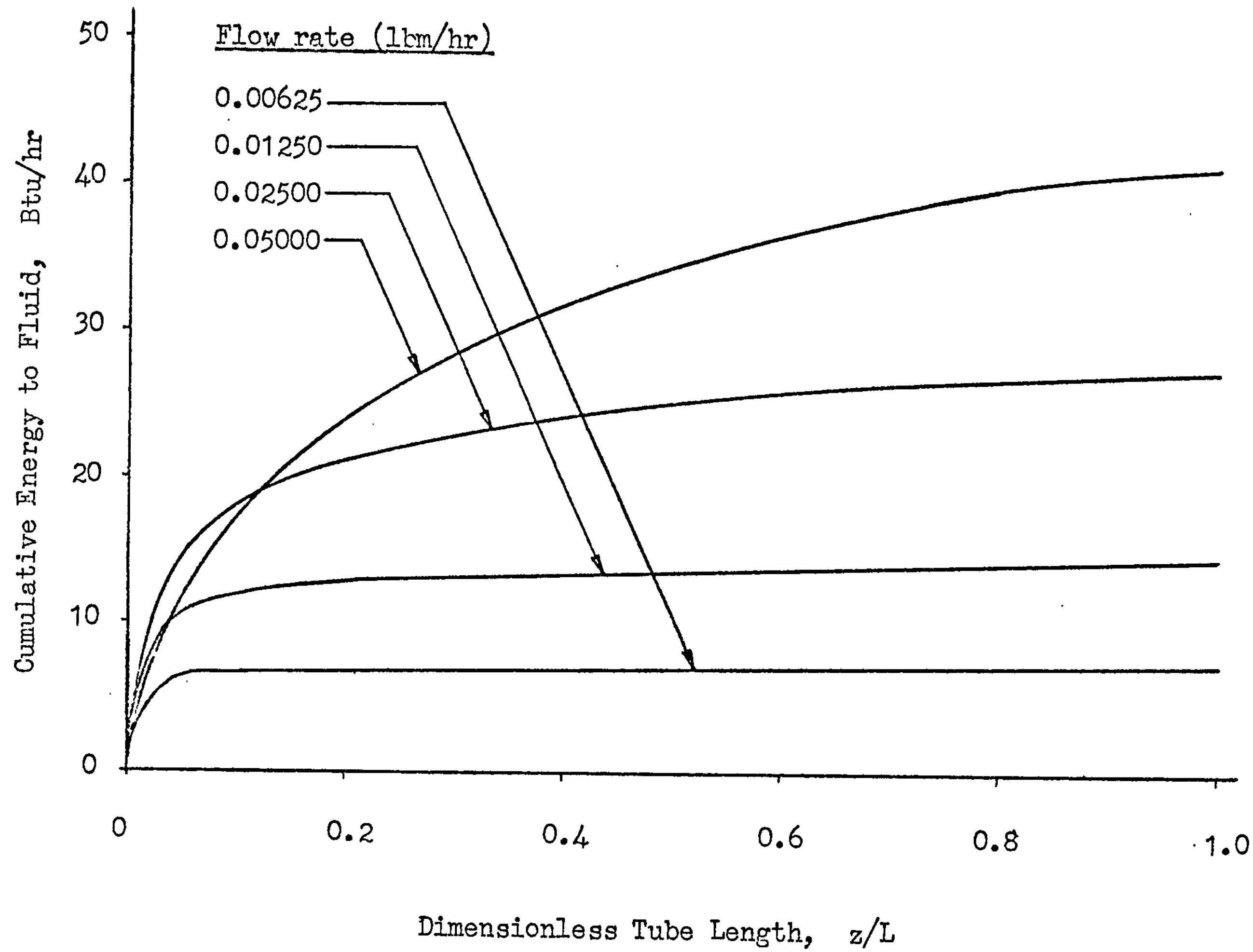

Figure 17. Cumulative Fluid Energy Absorption Profile for L/W = 0.5

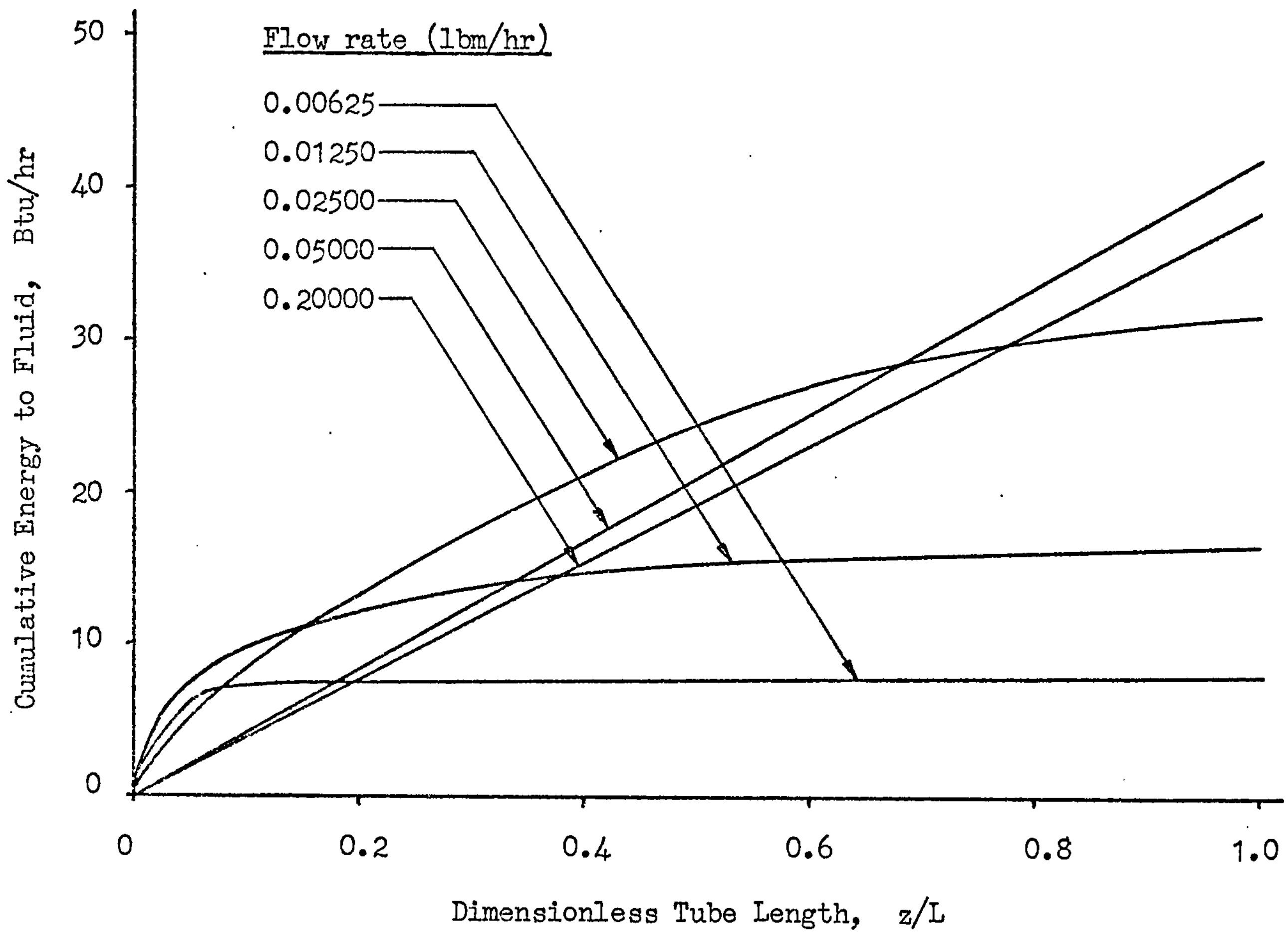

Figure 18. Cumulative Fluid Energy Absorption Profile for L/W = 12.5

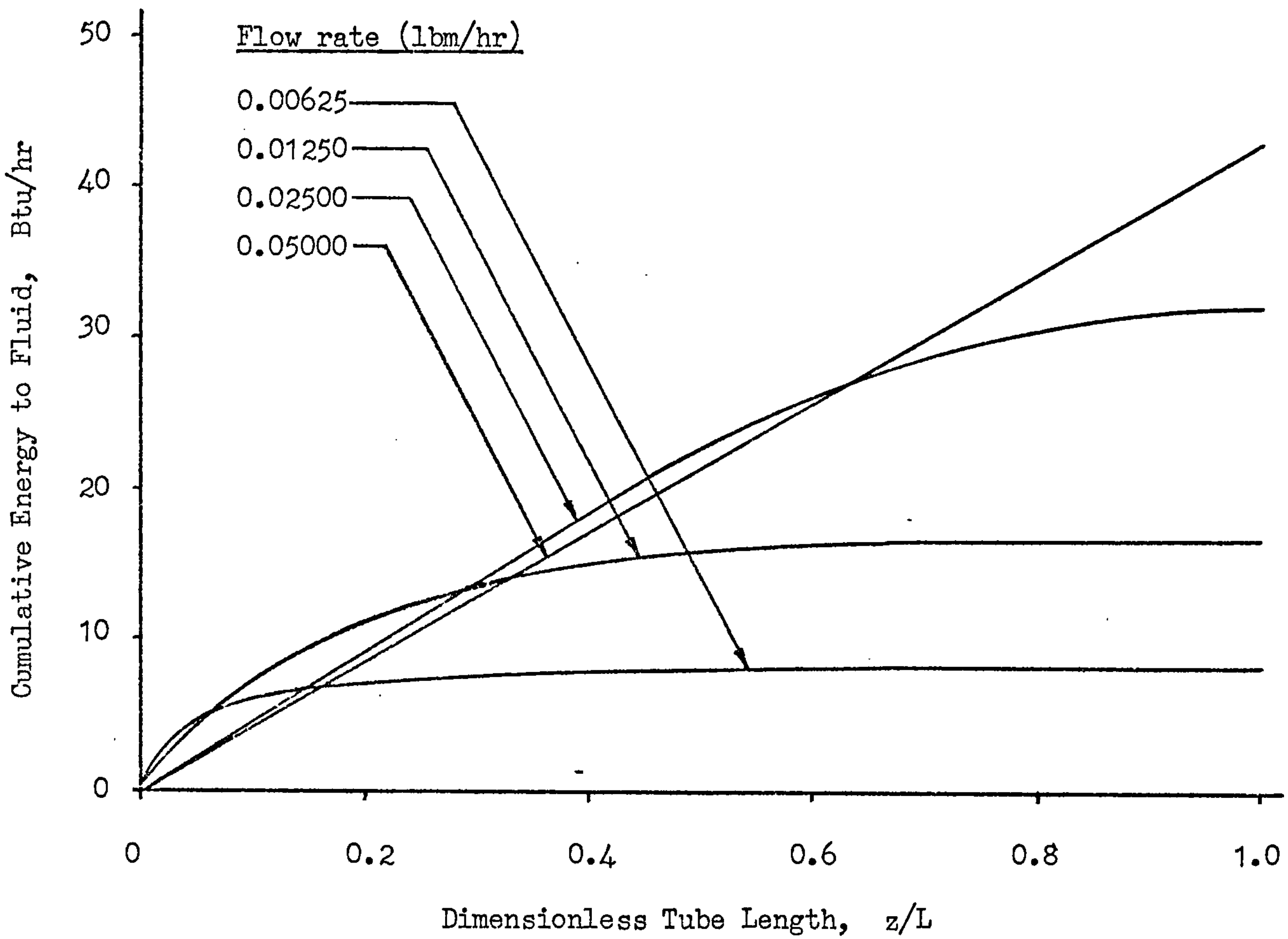

Figure 19. Cumulative Fluid Energy Absorption Profile for L/W = 50

L/W Ratio of Fin	Hydrogen Flow rate (lbm/hr)					
	0	0.00625	0.01250	0.0250	0.05000	0.20000
0.50	22.43	16.35	13.96	9.74	3.19	-
12.5	22.43	16.31	13.57	7.70	1.30	0.02
50.0	22.43	16.30	13.51	7.43	1.29	-

Table 1. Net Energy Transfer From Fin to Sink Measured in Btu/hr

As assessment of the effects of the assumptions made during the analytical formulation is in order to provide better perspective for interpretation of the results.

The assumption that all surfaces are diffuse is based on the fact that the area of all surfaces is equal and that the parallel flat plates are very closely spaced. Thus the possible error that may have been introduced is negligible.

Sample cases were run during the development of the computer program using constant fluid and material property data at an assumed value of -200°F. The results were then compared to the temperature-dependent cases shown herein. The use of temperature-dependent data resulted in a reduction of net heat leak to the sink of 15 to 20 per cent when compared to the results obtained using constant temperature property data.

The maximum error introduced by neglecting the radiant heat transfer from to to fin is less than 1% based on the tube to fin shape factor. The total surface area of the tube is less than 4% of that of the fin; and the tube to fin temperature profile is reasonably linear over the entire fin length. Thus the assumption of an adiabatic tube exterior surface should result in a maximum possible error of approximately 5%.

BIBLIOGRAPHY

1. Barron, R. Cryogenic Systems. New York: McGraw-Hill Co., 1966.

2. Lieblien, S. Analysis of Temperature Distribution and Radiant Heat Transfer Along a Rectangular Fin of Constant Thickness. NASA TN D-196, 1959.

3. Sparrow, E. M., Jonsson, V. K., and Minkowycz, W. J. Heat Transfer From Fin-Tube Radiators Including Longitudinal Heat Conduction and Radiant Interchange Between Longitudinally Nonisothermal Finite Surfaces. NASA TN D-2077, 1963.

4. Stockman, N. O., and Kramer, J. L. Effect of Variable Thermal Properties on One-Dimensional Heat Transfer in Radiating Fins. NASA TN D-1878, 1963.

5. Howell, J. R., and Siegel, R. Thermal Radiation Heat Transfer. Vol. II. NASA SP-164, 1969.

6. Jakob, M. Heat Transfer. Vol. II. New York: John Wiley & Sons, Inc., 1963.

7. Gaski, J. D., and Lewis, D. R. Chrysler Improved Numerical Differencing Analyzer: CINDA 3G. Chrysler TN-AP-67-287, 1967.

8. Touloukian, Y. S. Recommended Values of the Thermophysical Properties of Eight Alloys, Major Constituents and Their Oxides. Lafayette, Indiana: Purdue University, 1966.

9. Davis, M. L. "Silver Emissivity Survey." (Unpublished notes prepared in 1967, Houston, Texas)

10. Johnson, V. J. A Compendium of the Properties of Materials at Low Temperatures, Part I: Properties of Fluids. WADD TR 60-56, Wright-Patterson Air Force Base, Ohio: U. S. Air Force, 1960.

11. Hendricks, R. C., Graham, R. W., Hsu, Y. Y., and Medeiros, A. A. "Correlation of Hydrogen Heat Transfer in Boiling and Supercritical Pressure States." ARS Journal, 32, No. 2 (February, 1962), 244-252.